



LETTER

Airy-soliton interactions in self-defocusing media with PT potentials

To cite this article: Zhiwei Shi *et al* 2018 *EPL* **124** 14006

View the [article online](#) for updates and enhancements.

Airy-soliton interactions in self-defocusing media with PT potentials

ZHIWEI SHI^{1,5(a)}, HUAGANG LI², XING ZHU^{2,3} and ZHIGANG CHEN^{4,5}

¹ School of Electro-mechanical Engineering, Guangdong University of Technology - Guangzhou 510006, China

² Department of Physics, Guangdong University of Education - Guangzhou 510303, China

³ School of Photoelectric Engineering, Guangdong Polytechnic Normal University - Guangzhou 510665, China

⁴ The MOE Key Laboratory of Weak-Light Nonlinear Photonics, TEDA Applied Physics Institute and Physics of School, Nankai University - Tianjin 300457, China

⁵ Department of Physics and Astronomy, San Francisco State University - San Francisco, CA 94132, USA

received 10 August 2018; accepted 26 September 2018

published online 12 November 2018

PACS 42.65.Jx – Beam trapping, self-focusing and defocusing; self-phase modulation

PACS 42.65.Tg – Optical solitons; nonlinear guided waves

PACS 42.65.Wi – Nonlinear waveguides

Abstract – We investigate Airy-soliton interactions in self-defocusing media with PT potentials in one transverse dimension. We discuss different potentials in which the interacting beams with different phases are launched into the media at different separation distances. During interactions, there exist a primary collision region and a relaxation region accompanied by continuous interaction with the dispersed Airy tail. In the relaxation region, the beams exist as soliton-like and breathers-like propagation. The beam width and mean power are influenced by initial separation, phase shift and modulation depth of PT potentials. Especially, the collision distance decreases with the spatial beam separation and the mean power possesses sinusoidal dependence on the phase shift.

 Copyright © EPLA, 2018

Introduction. – Over the years, there has been an increasing interest in the study for which the diffraction can be eliminated through effective light-field regulation in many practical applications. Generally, there are two kinds of methods which can be used to offset the diffraction. One is to rely on the nonlinear (NL) effect in a medium. The formation of spatial solitons can be thought of as one of the most fundamental effects which give rise to localized structures that propagate unchanged, stabilized by the balance between the diffraction and the NL effect [1]. The other are non-diffracting beams in the free space. For instance, Airy optical beams, which exhibit self-accelerating, non-diffracting, and self-healing properties during propagation, were investigated theoretically and experimentally by Siviloglou *et al.* [2,3] for the first time in 2007. These novel properties of the Airy beams are ideally suited for various applications ranging from particle micromanipulation [4,5], self-bending plasma

channels [6], light bullets [7], optical interconnects [8], image signal transmission [9], super-resolution imaging [10], intrapulse Raman scattering [11], to name just a few.

The potential arising from combining both methods to investigate interactions of accelerating beams and solitons opens completely new perspectives of research. In the past decade, Airy beams in different NL media were widely studied, such as Kerr NL dielectrics [12–14], photorefractive media [15], non-local NL media [16,17], and quadratic media [12,18]. Because of the existence of nonlinearities, self-trapped beams can be realized with Airy-like beams/pulses [19,20] and self-accelerating solitary-like waves can also be found [13–15,18,21,22]. References [12–22] discussed non-diffracting beams all in uniform media. By considering modulated refractive index potentials (*i.e.*, the media are no longer uniform) a new degree of freedom is added to the system which brings about exciting new effects of the Airy beam propagation, which has already been considered in a few theoretical and experimental studies. Efremidis studied the propagation of Airy beams

^(a)E-mail: szwstar@gdut.edu.cn

in transversely linear index potentials [23]. In inhomogeneous media with a linear gradient index distribution, Moya-Cessa *et al.* demonstrated that an Airy beam propagates in a straight line [24]. Makris *et al.* studied non-diffracting accelerating paraxial optical beams in periodic potentials [25]. Hu *et al.* studied the behavior of Airy beams propagating from a NL medium to a linear medium [26]. Moreover, Dragana M. Jović *et al.* analyzed the influence of an optically induced photonic lattice on the acceleration of Airy beams [27,28]. However, the propagation dynamics of Airy beams in parity-time (PT)-symmetric potentials has thus far not been reported to our knowledge.

In optics, PT-symmetric potentials can be designed by introducing a complex refractive-index distribution $n(x) = n_R(x) + in_I(x)$, where $n_R(x) = n_R(-x)$, $n_I(x) = -n_I(-x)$, and x is the normalized transverse coordinate [29,30]. When nonlinearity is introduced, a novel class of NL self-trapped modes was found, and the interplay between the Kerr nonlinearity and the PT threshold was analyzed by Musslimani and co-workers [31]. Christodoulides' group presented closed-form solutions to a certain class of one- and two-dimensional NL Schrödinger equations involving potentials with broken and unbroken PT symmetry [32]. We also showed that defocusing Kerr media with PT-symmetric potentials can support one- and two-dimensional bright spatial solitons [29].

Moreover, the interactions between Airy pulse and temporal solitons at the same center wavelength [33] have been studied. The interaction of an accelerating Airy beam and a solitary wave has also been investigated for integrable and non-integrable equations governing NL optical propagation [34]. In the generic three-wave system, Mayteevarunyoo and Malomed have considered the collisions of truncated Airy waves and three-wave solitons [35]. Up to now, the interactions between an Airy beam and stable spatial beams in self-defocusing media with PT lattices have not been mentioned. When the two beams are placed in proximity to each other, with the Airy acceleration direction towards the soliton, interesting questions arise. For instance, will the soliton behave as an impenetrable barrier? Can the Airy probe control the soliton propagation parameters? How do the corresponding parameters affect the interaction of the beams? These questions are addressed in this paper. Specifically, we investigate the dynamics of two one-dimensional interacting beams along the propagation direction. We discuss the influence of different physical parameters on the beam interaction, including the initial spatial beam separation, phase difference, and amplitude ratio between the beams, the modulation depth and the width of PT potentials.

The theoretical model. – In a Kerr self-defocusing medium with PT-symmetric potentials, the scaled equation for the propagation of a slowly varying envelope $q(x, z)$ of the optical electric field in one transverse

dimension in the paraxial approximation is the normalized NL Schrödinger equation (NLSE) [31,32],

$$i\frac{\partial q}{\partial z} + \frac{1}{2}\frac{\partial^2 q}{\partial x^2} + R(x)q + \gamma|q|^2q = 0, \quad (1)$$

where z is the propagation distance which corresponds to the real distance $Z_r = zkw_0^2$, $k = 2\pi n_0/\lambda$, λ is the beam wavelength in the vacuum, w_0 is the input beam width, n_0 is the linear refractive index of media. $R(x) = V(x) + iW(x)$, and $V(x) = V_0 \operatorname{sech}^2(x/d)$ and $W(x) = W_0 \operatorname{sech}(x/d) \tanh(x/d)$ are the real and imaginary components of the complex PT-symmetric potential, respectively. V_0 and W_0 are the amplitudes of the real and imaginary parts. d denotes the width of PT potentials.

Obviously, when $R = 0$ and $\gamma = 0$, one of the accelerating solutions of eq. (1) is the well-known Airy function $q(x, z) = \operatorname{Ai}(x - z^2/4) \exp[i(6xz - z^3)/12]$ [2]. The ideal Airy beam does not exist in reality for its infinite energy. To make it finite-energy, an input Airy beam is defined by $q(x, 0) = \operatorname{Ai}(x) \exp(\alpha x)$, where $\alpha \geq 0$ is an arbitrary real decay parameter. If we assume $\gamma = -1$, the NLSE supports a PT soliton solution which can be described as $q(x, z) = q_{s0} \operatorname{sech}(x) \exp(i\rho \arctan(\sinh(x))) \exp(i\beta z)$ [32], where $\rho = W_0/3$, $q_{s0} = \sqrt{V_0 - w_0^2/9 - 2}$, and the propagation constant of the soliton $\beta = 1$. To investigate the interaction of an Airy beam and a PT soliton, we take the initial beam as a superposition of two beams

$$q(x, 0) = q_{s0} \operatorname{sech}(x) \exp(i\rho \arctan(\sinh(x))) + q_{A0} \operatorname{Ai}(x - D) \exp(\alpha(x - D)) \exp(i\theta), \quad (2)$$

where q_{A0} stands for the amplitude of the Airy beam. D is the initial Airy beam position with respect to the soliton (launched at $z = 0$), and θ controls the phase shift. When we vary these parameters, the soliton propagation must be affected. We demonstrate these interactions through numerical simulations using the Split Step Fourier Method. In our simulations, we choose a small truncation coefficient $\alpha = 0.03$, which guarantees that all the Airy beams have the same energy for a given q_{A0} value and only a small variation in peak intensity at the point of collision [33].

Numerical results of Airy beams in PT potentials. – Before discussing Airy-soliton interactions, we only consider the propagation of Airy beams in a defocusing nonlinear medium ($\gamma = -1$) with PT potentials. So, the input beam is $q(x, 0) = q_{A0} \operatorname{Ai}(x) \exp(\alpha x)$. We can see that Airy beams are divided into three parts due to the existence of PT potentials from figs. 1 and 2. One part may be soliton-like with small oscillations; When the solitary wave is hit by an Airy beam, it oscillates in both amplitude and position. The position oscillations are due to momentum exchange. The Airy beam gives the solitary wave momentum, but the potential traps the solitary wave, so it does not propagate away, but oscillates in the potential. The amplitude oscillations are a standard solitary wave behavior. If an NLS solitary wave is perturbed,

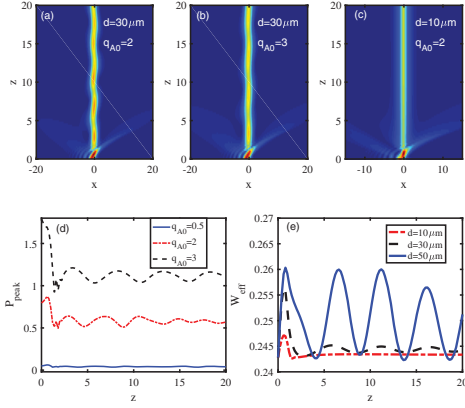


Fig. 1: (Color online) Intensity plots for the propagation of an Airy beam at (a) $q_{A0} = 0.5$, $d = 30\mu\text{m}$, (b) $q_{A0} = 2$, $d = 30\mu\text{m}$ and (c) $q_{A0} = 2$, $d = 10\mu\text{m}$. P_{peak} and W_{eff} as a function of the propagation distance z for different q_{A0} (d) and d (e) with $V_0 = 3$ and $W_0 = 0.3$.

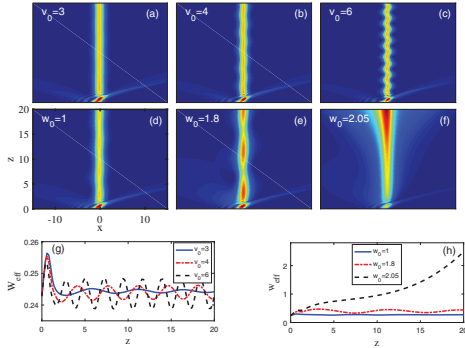


Fig. 2: (Color online) Intensity plots for the propagation of a Airy beam at (a) $V_0 = 3$, (b) $V_0 = 4$, and (c) $V_0 = 6$ with $W_0 = 0.3$ and (d) $W_0 = 1$, (e) $W_0 = 1.8$, and (f) $W_0 = 2.05$ with $V_0 = 3$. (g) The effective beam width W_{eff} via the propagation distance z for $W_0 = 0.3$. (h) W_{eff} via z with $V_0 = 3$. The other parameters are $q_{A0} = 2$ and $d = 30\mu\text{m}$.

it evolves to a steady state by oscillating in amplitude and width, shedding dispersive radiation in the process. The other part remains self-accelerating as the input Airy beam; The last part may be reflected waves. Here, we only pay attention to the first part. The influence of the amplitude of Airy beams and the width of PT potentials on their propagation properties is shown in fig. 1. The amplitude of the beam amplitude oscillation decreases with increasing q_{A0} , which can be seen from fig. 1(a) and (b). This can be illustrated by using Newtonian mechanics. q_{A0} is equivalent to the beam mass. When an Airy beam interacts with a PT potential, the amplitude of the beam amplitude oscillation must decrease with increasing q_{A0} for the same acting force of the PT potential. However, not only the peak intensity of the beam P_{peak} but also the oscillation amplitude of P_{peak} increases with q_{A0} , see fig. 1(d). This oscillation belongs to a position oscillation.

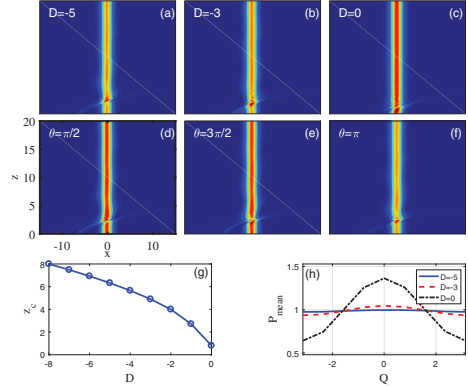


Fig. 3: (Color online) Airy-soliton interactions with an initial separation of (a) $D = -5$, (b) $D = -3$, and (c) $D = 0$ with $\theta = 0$ and (d) $\theta = \pi/2$, (e) $\theta = \pi$, and (f) $\theta = 3\pi/2$ with $D = -5$. (g) The collision distance Z_c as a function of parameter D . (h) The mean soliton intensity P_{mean} via θ for different D . The other parameters are $q_{A0} = 1$, $d = 30\mu\text{m}$, $V_0 = 3$, and $W_0 = 0.3$.

In addition, we also see that the oscillation amplitude of P_{peak} gradually becomes smaller during propagation because of the existence of beam decay. One can also find the effect of the width of PT potentials d on Airy beams. When d is smaller ($d = 10\mu\text{m}$), the soliton may form when $z > 8$ (fig. 1(c)). While d increases ($d = 30\mu\text{m}$), the beam oscillations (the soliton-like dynamics) shown in fig. 1(b) may appear. Figure 1(e) shows that the effective beam width $W_{eff} = \int_{-\infty}^{+\infty} |q|^2 / e^2$ varies with z for different d , where e is an exponential. We can find that W_{eff} is almost constant for $d = 10\mu\text{m}$, but it is oscillating when $d = 30\mu\text{m}$ and $d = 50\mu\text{m}$. Moreover, the amplitude of oscillation and W_{eff} increase with the width of PT potentials d . That is to say, as d is smaller, the Airy beam will be much more tightly localized because the binding force of PT potentials becomes stronger. Figure 2 illustrates how the amplitudes of the real and imaginary parts of PT potentials affect the beam propagation properties. Firstly, one can say that the amplitude of the oscillations of soliton-like largens and the oscillation period shortens from figs. 2(a)–(c) and fig. 2(g) when V_0 increases. Secondly, when we change W_0 , the properties of the beams are interesting. At $W_0 = 1$, the soliton-like may appear in fig. 2(d); At $W_0 = 1.8$, the breathers-like may take shape in fig. 2(e); At $W_0 = 2.05$, the beam may diffract in fig. 2(f). These results can be verified in fig. 2(h). The solitary wave solution [32] only exists for a fixed W_0 for a given amplitude q_{s0} related to W_0 . The solitary wave is just killed by large loss when W_0 is larger, so the beam diffracts.

Numerical results of Airy-soliton interactions in PT potentials. – For Airy-soliton interactions, the influence of the varied beam parameters on the beam propagation is discussed firstly. Figure 3 shows that two beams launch at different space separations D or different phase

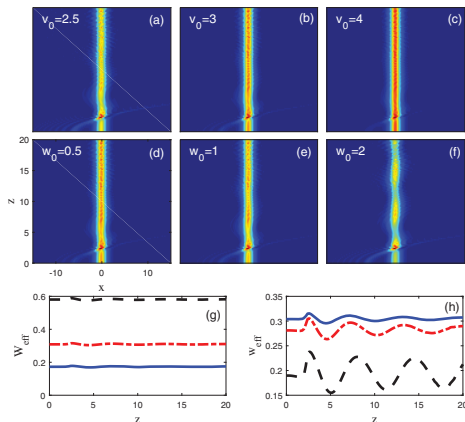


Fig. 4: (Color online) Intensity plots for the propagation of an Airy beam at (a) $V_0 = 2.5$, (b) $V_0 = 3$, and (c) $V_0 = 4$ with $W_0 = 0.3$ and (d) $W_0 = 0.5$, (e) $W_0 = 1$, and (f) $W_0 = 2$ for $V_0 = 3$. (g) The effective beam width W_{eff} via the propagation distance z for $V_0 = 2.5$ (solid blue line), $V_0 = 3$ (dash-dotted red line), and $V_0 = 4$ (dashed black line) at $W_0 = 0.3$. (h) W_{eff} via z for $W_0 = 0.5$ (solid blue line), $W_0 = 1$ (dash-dotted red line), and $W_0 = 2$ (dashed black line) at $V_0 = 3$. The other parameters are $q_{A0} = 0.5$, $\theta = 0$, $D = -5$, and $d = 30 \mu\text{m}$.

shifts θ for $q_{A0} = 1$, $d = 30$, $V_0 = 3$, and $W_0 = 0.3$. The propagating Airy beam decelerates to collide with the trailing soliton, so the interaction can be separated into two regimes of interest: the primary collision region between two beams (occurring at approximately $2 < z < 8$, for $D = -5$ in fig. 3(a)), and a relaxation region accompanied by continuous interaction with the dispersed Airy tail (occurring at $z > 8$). These are responsible for the different parameters such as space separation, phase shift, PT potential parameters, and soliton amplitude. During the primary collision, one cannot distinguish two beams which lose their identities due to interference throughout the collision region ($2 < z < 8$). However, as the Airy beam further moves towards later positions two beams reform and emerge having perturbed parameters. In addition, the Airy beam never completely crosses over the soliton, so the Airy-soliton interactions are classified as incomplete collisions [33]. From figs. 3(a)–(c), we can say that the collision distance Z_c lessens with D decreasing. Z_c is given by [33]

$$Z_c = 2\sqrt{Z_s - D} + Z_{peak}, \quad (3)$$

where Z_s is the soliton input position (in our case $Z_s = 0$) and Z_{peak} is the offset of the main Airy peak with respect to the space separation D . Z_{peak} is numerically calculated for a given truncation and space separation. For example, $Z_{peak} = 5$ for $\alpha = 0.03$ and $D = -5$, so $Z_c = 6.32$. Figure 3(g) verifies the relation of Z_c and D according to eq. (3). By establishing soliton power and background power from the maximum and minimum interference values, we can calculate the mean soliton

power P_{mean} far from collision. P_{mean} is charted for different initial Airy-soliton phases and separations at $q_{A0} = 1$, $d = 30$, $V_0 = 3$, and $W_0 = 0.3$ in fig. 3(h). It is obvious that P_{mean} increases with D . One can also find sinusoidal dependence on the initial Airy phase for all separations, illustrating an energy transfer between the beams during the primary collision.

Next, we change the modulation amplitudes V_0 and W_0 of PT potentials to find the effect of V_0 and W_0 on Airy-soliton interactions shown in fig. 4. From figs. 4(a)–(c) and (g), we find the behavior of soliton-like in the relaxation regions for different V_0 . The beam width of soliton-like W_{eff} increases with increasing V_0 . Figures 4(d)–(f) illustrate the change of the beam propagation with W_0 . The behaviors are similar to fig. 2(h) in the relaxation regions which can be seen in fig. 4(h) for different W_0 , which include soliton-like ($W_0 = 0.5$) and breathers-like ($W_0 = 2$).

Conclusion. – To conclude, we have investigated Airy-soliton interactions in self-defocusing nonlinear media with PT potentials by using the numerical simulations with the split-step Fourier method. If we only consider the propagation of Airy beams in a defocusing nonlinear medium, the propagation dynamics can be described and divided into three parts due to the existence of PT potentials: one part is soliton-like propagation with small oscillations; the other part remains self-accelerating as the input Airy beam; the last part may be associated with reflected waves. The amplitude and period of the oscillations may be affected by input beam amplitude and PT potential parameters. We find that soliton-like and breather-like dynamics can be produced during propagation. For Airy-soliton interactions, the propagating Airy beam can decelerate to collide with the trailing soliton, so the interaction can be separated into two regimes of interest: the primary collision region between the beams and a relaxation region accompanied by continuous interaction with the dispersed Airy tail. In the relaxation region, the behaviors of soliton-like and breather-like dynamics can also be observed. The beam width and mean power are influenced by space separation, phase shift and modulation depth of PT potentials. More interestingly, the collision distance becomes smaller when spatial separation between two beams is smaller, and the mean soliton-like power exhibits sinusoidal dependence on the initial Airy phase. The numerical simulations presented in this paper motivate an experimental implementation of interactions of Airy beams and solitons in PT potentials which can be realized through a judicious inclusion of index guiding and gain/loss regions in optics [29,36]. Controlling the propagation behavior of light with light itself is the key requirement to realize new all-optical guiding and switching architectures, so these experiments, which is to tailor the transverse acceleration of optical Airy beams using PT potentials and solitary waves, may enable new configurations for all-optical interconnections.

Also other classes of self-accelerated optical beams can be controlled using the presented ideas and methods.

* * *

This project was supported by the National Natural Science Foundation of China under (Grant No. 11774068), Natural Science Foundation Guangdong Province of China (Grant No. 2016A030313747), and by the National Key RD Program of China (2017YFA0303800).

REFERENCES

- [1] CHEN Z. G., SEGEV M. and CHRISTODOULIDES D. N., *Rep. Prog. Phys.*, **75** (2012) 086401.
- [2] SIVIOGLOU G. A. and CHRISTODOULIDES D. N., *Opt. Lett.*, **32** (2007) 979.
- [3] SIVIOGLOU G. A., BROKY J., DOGARIU A. and CHRISTODOULIDES D. N., *Phys. Rev. Lett.*, **99** (2007) 213901.
- [4] BAUMGARTL J., MAZILU M. and DHOLAKIA K., *Nat. Photon.*, **2** (2008) 675.
- [5] SCHLEY R., KAMINER I., BEKENSTEIN R., GREENFIELD E., LUMER Y. and SEGEV M., *Nat. Commun.*, **5** (2014) 5189.
- [6] POLYNKIN P., KOLESIK M., MOLONEY J. V., SIVIOGLOU G. A. and CHRISTODOULIDES D. N., *Science*, **324** (2009) 229.
- [7] CHONG A., RENNINGER W. H., CHRISTODOULIDES D. N. and WISE F. W., *Nat. Photon.*, **4** (2010) 103.
- [8] WIERSMA N., MARSAL N., SCIAMANNA M. and WOLFERSBERGER D., *Opt. Lett.*, **39** (2014) 5997.
- [9] LIANG Y., HU Y., SONG D., LOU C. B., ZHANG X. Z., CHEN Z. G. and XU J. J., *Opt. Lett.*, **40** (2015) 5686.
- [10] JIA S., VAUGHAN J. C. and ZHUANG X., *Nat. Photon.*, **8** (2014) 302.
- [11] HU Y., TEHRANCHI A. and WABNITZ S., *Phys. Rev. Lett.*, **114** (2015) 073901.
- [12] KAMINER I., SEGEV M. and CHRISTODOULIDES D. N., *Phys. Rev. Lett.*, **106** (2011) 213903.
- [13] LOTTI A., FACCIO D., COUAIRO A., PAPAOGLOU D. G., PANAGIOTOPOULOS P., ABDOLLAHPOUR D. and TZORTZAKIS S., *Phys. Rev. A*, **84** (2011) 021807.
- [14] KAMINER I., NEMIROVSKY J. and SEGEV M., *Opt. Express*, **20** (2012) 18827.
- [15] JIA S., LEE J., FLEISCHER J. W., SIVIOGLOU G. A. and CHRISTODOULIDES D. N., *Phys. Rev. Lett.*, **104** (2010) 253904.
- [16] BEKENSTEIN R. and SEGEV M., *Opt. Express*, **19** (2011) 23706.
- [17] ZHOU G., CHEN R. and RU G., *Laser Phys. Lett.*, **11** (2014) 105001.
- [18] DOLEV I., KAMINER I., SHAPIRA A., SEGEV M. and ARIE A., *Phys. Rev. Lett.*, **108** (2012) 113903.
- [19] ABDOLLAHPOUR D., SUNTSOV S., PAPAOGLOU D. G. and TZORTZAKIS S., *Phys. Rev. Lett.*, **105** (2010) 253901.
- [20] PANAGIOTOPOULOS P., PAPAOGLOU D. G., COUAIRO A. and TZORTZAKIS S., *Nat. Commun.*, **4** (2013) 2622.
- [21] ELLENBOGEN T., VOLOCH-BLOCH N., GANANY-PADOWICZ A. and ARIE A., *Nat. Photon.*, **3** (2009) 395.
- [22] HU Y., SUN Z. and BONGIOVANNI D., *Opt. Lett.*, **37** (2012) 3201.
- [23] EFREMIDIS N. K., *Opt. Lett.*, **36** (2011) 3006.
- [24] CHÁVEZ-CERDA S., RUIZ U., ARRIZÓN V. and MOYACESSA H. M., *Opt. Express*, **19** (2011) 16448.
- [25] MAKRIS K. G., KAMINER I., EL-GANAINY R., EFREMIDIS N. K., CHEN Z., SEGEV M. and CHRISTODOULIDES D. N., *Opt. Lett.*, **39** (2014) 2129.
- [26] HU Y., HUANG S., ZHANG P., LOU C., XU J. and CHEN Z., *Opt. Lett.*, **35** (2010) 3952.
- [27] PIPER A., TIMOTIJEVIĆ D. V. and JOVIĆ D. M., *Phys. Scr.*, **T157** (2013) 014023.
- [28] DIEBEL F., BOKIĆ B. M., BOGUSLAWSKI M., PIPER A., TIMOTIJEVIĆ D. V., JOVIĆ D. M. and DENZ C., *Phys. Rev. A*, **90** (2014) 033802.
- [29] MUSSLIMANI Z. H., MAKRIS K. G., EL-GANAINY R. and CHRISTODOULIDES D. N., *Phys. Rev. Lett.*, **100** (2008) 030402.
- [30] WANG H. and WANG J. D., *Opt. Express*, **19** (2011) 4030.
- [31] MUSSLIMANI Z. H., MAKRIS K. G., EL-GANAINY R. and CHRISTODOULIDES D. N., *J. Phys. A*, **41** (2008) 244019.
- [32] SHI Z. W., JIANG X. J., ZHU X. and LI H. G., *Phys. Rev. A*, **88** (2011) 053855.
- [33] RUDNICK A. and MAROM D. M., *Opt. Express*, **19** (2011) 25570.
- [34] ASSANTO G., MINZONIB A. A. and SMYTH N. F., *Wave Motion*, **52** (2015) 183.
- [35] MAYTEEVARUNYOO T. and MALOMED B. A., *J. Opt.*, **19** (2017) 085501.
- [36] RÜTER C. E., MAKRIS K. G., EL-GANAINY R., CHRISTODOULIDES D. N., SEGEV M. and KIP D., *Nat. Phys.*, **6** (2017) 192.